Physicochem. Probl. Miner. Process., 57(1), 2021, 284-293

http://www.journalssystem.com/ppmp

Physicochemical Problems of Mineral Processing

ISSN 1643-1049

Received November 18, 2020; reviewed; accepted December 25, 2020

Significance of reagents addition sequence on iron anionic reverse flotation and their adsorption characteristics using QCM-D

Ying Hou [1], Ahmed Sobhy [2,3], Yue Wang [4]

[1] School of Mining Engineering, University of Science and Technology Liaoning, Anshan 114051, China

[2] School of Resources and Environmental Engineering, Shandong University of Technology, Zibo, 255049, China

[3] Minerals Technology Department, Central Metallurgical R&D Institute, Helwan, Cairo, 11421, Egypt

[4] School of Chemical Engineering, University of Science and Technology Liaoning, Anshan 114051, China

Corresponding author: asobhy@qq.com (Ahmed Sobhy)

Abstract: To explore the influence of reagents addition sequence of the pH regulator and the starch depressant on the anionic reverse flotation of iron oxide, flotation conditional experiments were performed on mixed low-intensity and high-gradient magnetic concentrates which is the flotation feed acquired from the iron processing plant. Besides, quartz crystal micro-balance with dissipative (*QCM-D*) was conducted to detect the adsorption phenomena of the flotation reagent on iron oxide sensors at different addition orders. The outcomes showed that the flotation performance using the pH regulator prior to the depressant was the best. For example, at 1.6 kg/Mg starch dosage, the recovery and separation efficiencies were improved by 18.3% and 21.2%, respectively, with keeping the concentrate Fe grade as high as 69.5%. Also, *QCM-D* frequency shifted by -41 Hz from 17 Hz to -24 Hz with increased dissipation from -2.6 x 10^{-6} to 8.2 x 10^{-6}, indicating an increase in the mass of slightly-rigid starch adsorption layer on the surface of iron oxide under a strong alkaline condition with adsorption density of about 0.46 mg/cm^2. On the other hand, under weak alkaline conditions, starch was adsorbed, and then the starch was desorbed upon the addition of the strong alkaline solution. Whereas, adding the pH modifier to create a strong alkaline condition enhanced the starch adsorption significantly with coordination and hydrogen bonds, and prevented the following adsorption of the anionic collector for more efficient reverse flotation of iron oxide minerals.

Keywords: iron oxide, adsorption, pH modifier, starch, reverse flotation, QCM-D

1. Introduction

In recent years, with the successful development and application of new tools, new reagents and new processes, iron ore processing technology has made a breakthrough, developing a joint selection process represented by stage grinding, magnetic separation, and anionic reverse flotation to reach the world's leading level (Ma, 2012). Iron ore flotation started in 1931 via a direct anionic flotation route (Ma, 2012), and the reverse anionic flotation has been established for its higher economic performance in the early 1960s (Filippov et al., 2014; Veloso et al., 2018). Reverse anionic flotation is the most widely used flotation route, in which starch is added as a depressant for iron oxide particles, Ca^{2+} as an activator, and anionic collector as a collector for quartz at a high pH value (Ma, 2012; Quast, 2017; Yang and Wand, 2018). At the high pH value of 11-12, the repulsive electrostatic forces with negative charge between iron oxide and quartz particles are strong enough to eliminate the heterocoagulation phenomenon between iron oxide and quartz particles. Thus, the selective adsorption of starch on iron oxide particles could be more significant (Bhagyalaxmi et. al, 2013; Lu et al., 2017). However, the mechanism of depressant adsorption on iron minerals is not clear enough. Thus, the application of quartz crystal micro-balance with dissipation (*QCM-D*) (Sakai, 2019), atomic force microscope (*AFM*) (Butt et al., 2005), and zeta potential, combined with single mineral flotation may be useful tools for the adsorption

DOI: 10.37190/ppmp/131950

mechanism investigation. Alternatively, total organic carbon analyser (*TOC*) is applied to measure the concentration of remaining total dissolved organic carbon in supernatants after adsorption on mineral particles, while *QCM-D* is more beneficial in studying the adsorption phenomena of any chemical compounds on a mineral surface in real time (Wang et al., 2014). *QCM-D* provides real-time data about viscoelastic characteristics of the adsorbed layer, such as density, elasticity, viscosity, mass, thickness, and kinetics of molecular interactions (Saftic et al., 2018).

Others studied the depression properties of flotation agents on iron minerals, and it was found that starch has a strong depression effect on iron minerals (Yang et al., 2017; Tohry et al., 2019). Besides, the researchers have done a lot of research on the adsorption between flotation reagents and both iron minerals and quartz, but mainly for the comparison of flotation reagents (Vijayakumar et al., 2010), but the reagents addition sequence of the regulator and depressant in reverse flotation of iron ore has not studied yet. Thus, this study aimed to investigate the effects of pH regulator and depressant addition sequence in the reverse flotation performance and applies *QCM-D* to study the adsorption characteristics to lay a theoretical foundation for the efficient reverse flotation of iron minerals.

2. Materials and methods

2.1. Materials

The experimental sample was a representative flotation feed, which was a mixture of low-intensity and high-gradient magnetic concentrates obtained from Anqian Processing Plant of Anshan Iron and Steel Co., Ltd., Anshan, Liaoning, China. The as-received sample was dried to remove the moisture contents, split into small portions, and sealed in plastic bags for later usages.

The experimental reagents; corn starch, purity≥98%, and sodium hydroxide, purity≥97%, were purchased from Shanghai Aladdin Biochemical Technology Co., Ltd. Starch is a typical depressant of iron minerals in reverse flotation, and the chemical form of starch is $(C_6H_{10}O_5)_n$ polymer with a molecular weight of 162.14 g/mol. The rest of the flotation reagents such as lime (CaO) as a quartz activator, and anionic TD-II as a quartz collector are commercial products acquired from the Anqian processing plant of Anshan Iron and Steel Co., Ltd and were used as received (Tao et al., 2021).

2.2. Sample characterization

The mineralogical composition of the experimental sample was characterized qualitatively using the coupling X-ray diffraction (Bruker D8 *XRD*) diffractometer. The scan range from 10° to 100° with 0.01° step size, 1°/min scanning speed, and 40 kV accelerating voltage was used. The *XRD* pattern results are shown in Fig. 1, which indicates that the major minerals in the flotation feed were magnetite, hematite, and quartz. X-ray fluorescence (*XRF*) analysis was also conducted to confirm that the main constituents of the tested sample, and the results are presented in Table 1. Table 2 shows also the quantitative mineralogical analysis data obtained by mineral liberation analyzer *MLA* 650F (FEI, USA) (Sylvester, 2012), which identifies that the main iron minerals were magnetite, hetero-iron, and hematite with the distribution of 80.05%, 9.27%, and 10.15%, respectively, with a low amount of silica and carbonate.

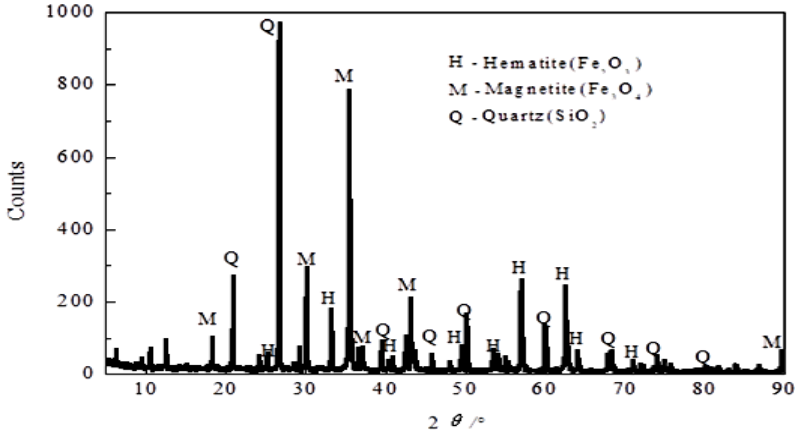

Fig. 1. X-ray diffraction analysis of the experimental samples

Table 1. X-ray fluorescence analysis of the representative sample

Fe	Na_2O	MgO	Al_2O_3	SiO_2	K_2O	CaO	P	S	Cu	Pb	Zn	Co	BaO
48.1335	0.0368	0.5973	0.1065	50.2756	0.0192	0.5296	0.0934	0.1082	0.0146	0.03	0.016	0.0016	0.1377

Table 2. Phase analysis of the experimental sample using *MLA*

Phase	Total iron	Magnetite	Hetero-iron	Hematite	Silica	Carbonate
Content (%)	47.47	38.00	4.40	4.82	0.15	0.10
Distribution (%)	100.00	80.05	9.27	10.15	0.32	0.21

2.3. Experimental methods

Laboratory flotation experiments were conducted using XFG-ⅡI flotation machine with a 1.5 dm^3 cell using two routes according to Fig. 2(a-b) at 35°C temperature, 33.3% solids, and 1920 rpm rotor speed to examine the effect of the reagents addition sequence on the flotation performance. The fixed conditions such as the temperature and percent solids, rotor speed, conditioning time, and flotation time were selected based on the actual industrial anionic reverse flotation of iron at Anqian processing plant of Anshan Iron and Steel Co., Ltd.

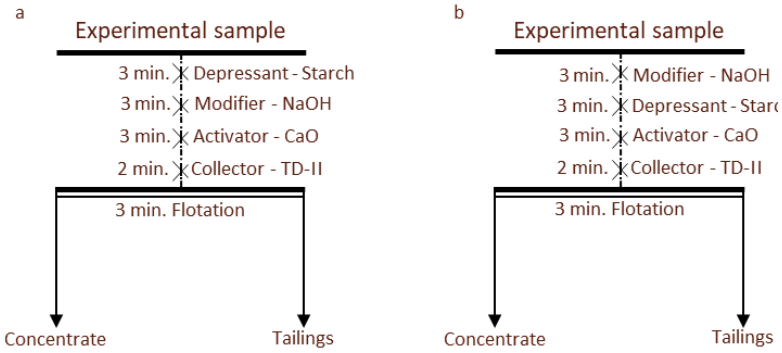

Fig. 2. Process flow diagrams of flotation experiments with different reagents addition sequences

Unless otherwise stated, the sample suspensions pH was adjusted to 11.5 by adding pH regulators for 3 min before or after adding the starch as a depressant for iron minerals according to the reagents addition sequence given in Fig. 2(a-b). The starch was mixed for 3 min. Then, 0.4 g/Mg CaO was added for 3 min to activate the quartz to accommodate the adsorption of 0.76 g/Mg TD-II anionic collector for 2 min. The flotation time was kept constant at 3 min. The froth was scraped manually by using a plastic blade. The concentrates and tailings were dried, weighed, and analyzed for the total iron grade and recovery.

The separation efficiency (Eq. 1) was estimated by applying the formula proposed by Fleming and Stephen (Zhang et al., 2018).

$$E_{fs} = \varepsilon \frac{\beta - \alpha}{\beta_{max} - \alpha} \quad (1)$$

where E_{fs} is the separation efficiency, ε is the recovery rate, β is the concentrate grade, β_{max} is the maximum theoretical grade, and α is the feed grade. The recovery rate is the percentage of total iron recovered in the product from the feed.

2.3. Quartz crystal microbalance (*QCM-D*) measurements

The quartz crystal microbalance (*QCM-D*) was conducted to study the adsorption using two channels of the four-channel Q-Sense Analytic from Biolin Science, Sweden. The adsorption temperature was set at 35°C, and the pH of the starch solution was 9.19 and 11.68, with a concentration of 60 mg/dm^3. NaOH solution was prepared at a pH 11.68. *QCM-D* measurements were carried out at high temperatures to represent the actual industrial anionic reverse flotation of iron, which was accomplished at 35°C (Tao et al., 2021).

The *QCM-D* sensors coated with iron oxide were used after cleaning with ethanol and 2% Hellmanex liquid, rinsing with distilled water, and blow-drying with nitrogen. IPC-N 4 channels high precision peristaltic pump (Ismatec, Switzerland) was used with 0.2 cm^3/min flow rate to feed distilled water to establish a stable baseline at zero frequency and dissipation shifts. Then, to estimate the adsorption phenomena and the reagent addition sequences, NaOH and starch solutions were fed into two different channels until the adsorption on the sensors indicated by curves of frequency and dissipation shifts reached a stable plateau. Then, each solution was introduced to the other flow module until a new equilibrium was achieved.

The frequency shift (Δf) of the oscillating iron oxide sensor is directly proportional to its mass change (Δm) as shown in Eq. 2 (Konradi et al., 2012; Saftic et al., 2018).

$$\Delta m = -C\frac{\Delta f}{n} \tag{2}$$

where n is the overtone number which is 3 for the third overtone, and C is a constant equal to 17.7 ng/(cm^2 Hz) for 4.95 MHz iron oxide oscillating sensor. Therefore, nanogram-scale adsorption is detected precisely because of the accurate detection of 4.95 MHz within a precision of 0.01 Hz using *QCM-D* could be established very easily.

3. Results and discussion

In reverse anionic flotation of iron oxide minerals, there are four kinds of chemical reagents applied to the flotation slurry for different roles (Ma, 2012), including NaOH, starch, CaO, and fatty acids. NaOH is used as a pH regulator to adjust the pH value of the slurry to about 11.5 to enrich the surface charges on the oxide minerals and slime coating for strong repulsion that de-sliming is no longer needed. Starch is engaged as a depressant for iron oxide minerals (Veloso et al., 2018). CaO is mixed as an activator for quartz mineral, which is converted into $Ca(OH)^+$, the most effective form for activation obtained at the strong alkaline conditions for efficient subsequent processes (Ren and Sun, 2018). Anionic collectors such as fatty acids are employed as collectors of activated quartz.

3.1. Effects of depressant and regulator addition sequence at varying starch dosage

According to the test process in Fig. 2a, the specific dosage of starch was added at about 9 pH for 3 min. Then, NaOH as a pH regulator was added to adjust the slurry pH value at about 11.5. Then, quartz particles were activated with 0.4 kg/Mg CaO to adsorb 0.76 kg/Mg TD-II anionic collector, and the reverse flotation results are shown in Figs. 3 and 4.

The results presented in Fig. 3 shows that both Fe grade and recovery improved with the increasing the starch dosage up to 0.8 kg/Mg. Further increase in starch dosage increased Fe grade with a slight decrease in Fe recovery. Similarly, Fig. 4 shows that the increasing in the starch dosage from 0.3 kg/Mg to 0.8 kg/Mg significantly increased the separation efficiency from 19% to 51%, and then the separation

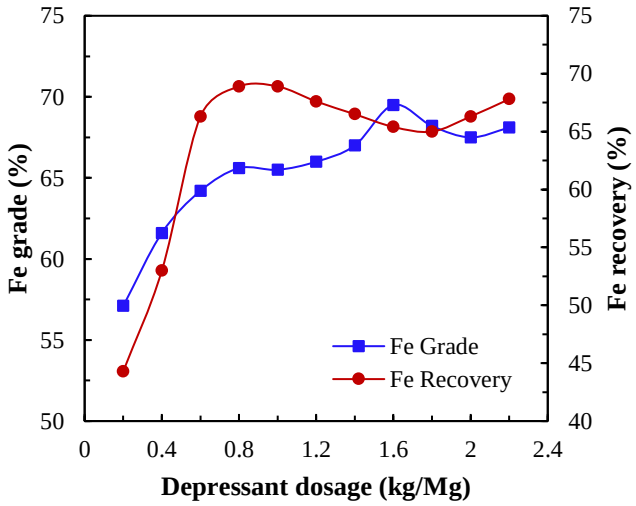

Fig. 3. Effect of depressant dosage on flotation recovery

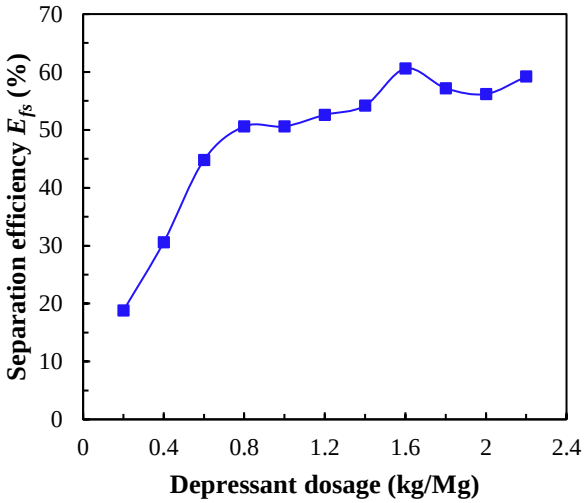

Fig. 4. Effect of depressant dosage on separation efficiency

efficiency increased to 59% with the extra increase in the starch dosage from 0.8 kg/Mg to 1.6 kg/Mg. The higher starch dosage of more than 1.6 kg/Mg showed no any additional improvement. Furthermore, at 1.6 kg/Mg starch dosage, Fe grade, Fe recovery, and separation efficiency were obtained as 69.2%, 65.4%, and 61% respectively.

3.2. Effects of regulator and depressant addition sequence at varying starch dosage

According to the test process in Fig. 2b, NaOH as a pH regulator was added to adjust the slurry pH value at about 11.5. Then a specific dosage of the starch solution was added to the slurry as a depressant. Then, the subsequent process was activating the quartz with 0.4 kg/Mg CaO to accommodate the adsorption of 0.76 kg/Mg TD-II anionic collector, and the reverse flotation results are shown in Fig. 5 and Fig. 6.

The results shown in Fig. 5 indicate that the starch dosage had significant effects on Fe grade and Fe recovery. The grade and recovery increased to 69.5% and 83.5%, respectively, with increasing the starch dosage from 0.3 kg/Mg to 1.6 kg/Mg. The additional increase in the starch dosage to 2.3 kg/Mg reduced Fe grade to 67.4% with a slightly higher recovery of 84.9%.

Figure 6 shows the effects of starch dosage on the separation efficiency. The separation efficiency improved from 12% to 82% with increasing the starch dosage from 0.3 kg/Mg to 1.6 kg/Mg and then decreased to 77% with increasing the starch dosage to 2.3 kg/Mg. Thus, at 1.6 kg/Mg starch dosage, Fe grade, Fe recovery, and separation efficiency were obtained as 69.5%, 83.5%, and 82% respectively.

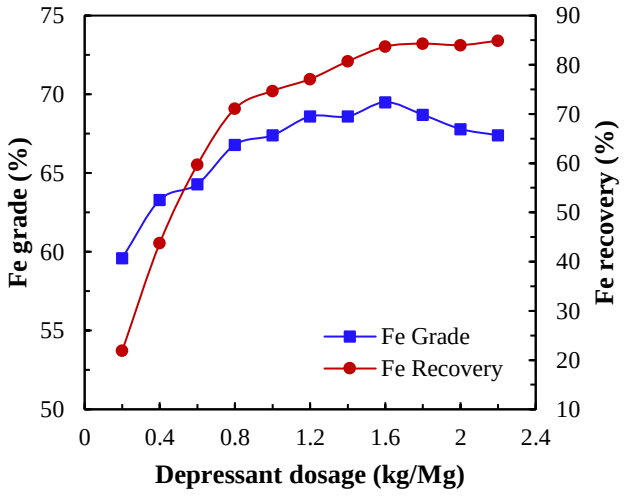

Fig. 5. Effect of depressant dosage on flotation recovery

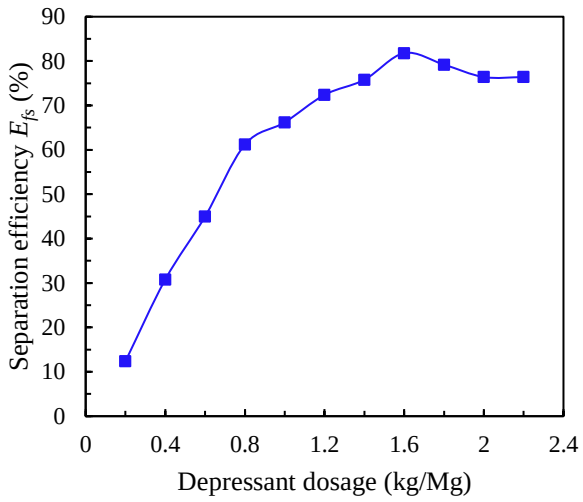

Fig. 6. Effect of depressant dosage on separation efficiency

3.3. Effects of the addition sequence on reverse flotation efficiency

Comparing the effects of the reagents addition sequence as shown in Fig. 7, indicates that using the pH regulator to adjust the pH value at 11.5 before the addition of starch showed a superior enhancement in the separation efficiency significantly at starch dosage above 0.6 kg/Mg. For example, at 1.6 kg/Mg starch dosage, the separation efficiency was improved by about 21%.

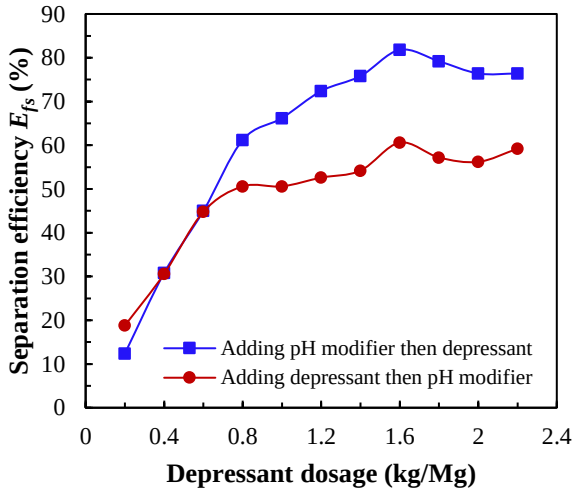

Fig. 7. Effects of addition sequence of regulator and depressant on the separation efficiency of reverse flotation

3.4. Adsorption mechanism of starch on the iron oxide (magnetite) surface

The starch molecules adsorption mechanism before and after adding a strongly alkaline solution on the iron oxide surface was identified by conducting *QCM-D*. The starch solution (9.19-11.68 pH, 60 mg/dm^3 concentration) and sodium hydroxide solution (11.68 pH) were fed on iron oxide crystal sensors which resulted in frequency changes (Δf) and energy dissipation changes (ΔD) as shown in Fig. 8, Fig. 9, andFig. 10. From changes in the vibration frequency and the associated energy dissipation of the iron oxide chip, *QCM-D* can provide some information about the properties of the adsorbed film and the amount of adsorption to the sensor surface (Hodges et al., 2020). *QCM-D* set-up shown in Fig. 8 is used to in-situ track the mass changes that could occur on the surfaces of the sensor at the nanogram-scale. Fig. 8 shows that the reagent solution is pumped from the sample holder at the right, via the measurement chamber to the waste container at the left. The real-time presentation of what happens on the surfaces such as kinetics, swelling, adsorption, desorption, etc, is displayed as frequency and dissipation shifts (Δf and

ΔD). The negative frequency shift indicates the adsorption of starch molecules on the iron oxide surface, which the increase in the dissipation shift reflects the less rigidity adsorption layer as shown in Fig. 8.

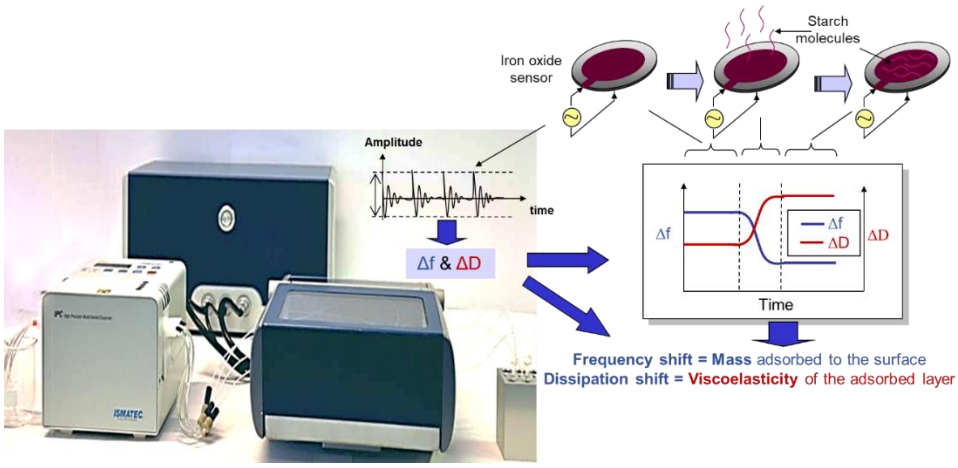

Fig. 8. Quartz crystal microbalance (*QCM-D*) set-up and illustration of starch adsorption mechanism on iron oxide sensor

Fig. 9 shows the frequency and dissipation shifts with time as a result of interactions of starch followed by NaOH with the surface of iron oxide studied by *QCM-D*. The frequency shift (*Δf*) of the iron oxide chip by -23 Hz toward lower frequency values indicated an increase in mass on its surface as a result of starch adsorption under weak alkaline conditions (9.19 pH). Also, the slight dissipation shift *ΔD* by about 1.75 x10^{-6} indicated a thinner, denser, and rigid adsorption layer.

Fig. 9. also shows that *Δf* increased from -23 Hz to 62 Hz with the addition of strong alkaline sodium hydroxide solution (11.68 pH) indicating the desorption of starch of the surface of iron oxide and the adsorption of a large number of hydroxyl ions, which started by decreasing the rigidity of the starch-adsorbed layer as specified by increasing *ΔD* from 1.75 x10^{-6} to 6.5 x10^{-6}. Then, the dissipation shift showed a downward trend with the further addition of the strong alkaline sodium hydroxide solution over time reaching a zero value. Thus, the addition of starch solution before the strong alkaline solution reduces the adsorption of starch on the iron oxide particles in the reverse flotation process, which in consequence reduces the separation efficiency.

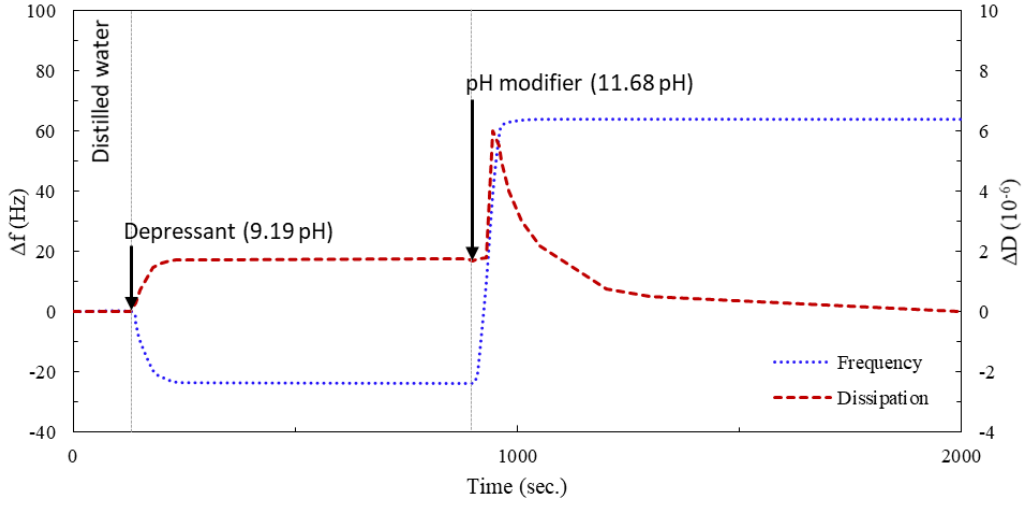

Fig. 9. Frequency and dissipation shafts with time as a result of interactions of starch depressant (starch) followed by pH modifier (NaOH) with the surface of iron oxide studied by *QCM-D*

Fig. 10 shows the frequency and dissipation shifts with time as a result of interactions of pH modifier (NaOH) followed by starch depressant (starch) with the surface of iron oxide studied by *QCM-D*. The frequency shift showed an upward trend after adding a strong alkaline sodium hydroxide solution. The

increase in the frequency shift from 0 to 17 Hz indicates a decrease in mass on the surface of the iron oxide by adding NaOH due to the adsorption of hydroxyl ions (Ishikawa et al., 1997). Ishikawa et al. (1997) also found that iron oxide especially hematite could dissolution forming $Fe(OH)_3$ with increasing the concentration of NaOH. On the other hand, the dissipation shift showed a downward trend with decreasing in mass on the surface of iron oxide.

Fig. 10 shows also the frequency shift decreased from 17 Hz to -24 Hz by adding starch solution at strong alkaline conditions (11.68 pH) which shows an increase in the mass on the surface of iron oxide. The dissipation shift increase from -2.6 x 10^{-6} to 8.2 x 10^{-6} showing a slightly rigid adsorption layer of starch on the iron oxide surface. The higher dissipation shifts up to 8.2 x 10^{-6} could be due to the swelling of starch molecules adsorbed on the surface of iron oxide (Bouchet-Spinelli et al., 2013; Clegg et al., 2019). The rigidity is because starch molecules cover the surface of iron oxide through reactions with the surface hydroxyl groups of iron oxide particles and the hydroxyl group from the polysaccharide molecules of the starch (Liuyin et al., 2009; Zhang et al., 2011) in addition to the coordination bonds between Fe^{3+} of iron oxide surface and the hydroxyl groups of starch (Weissenborn et al., 1995).

The comparison between the two cases of reagent addition sequence in terms of mass changes on the surface of iron oxide confirms that pH regulator should be used before the addition of starch molecules as shown in Fig. 11. Fig. 11 indicates that Δm increased to 0.43 mg/cm^2 due to starch adsor-

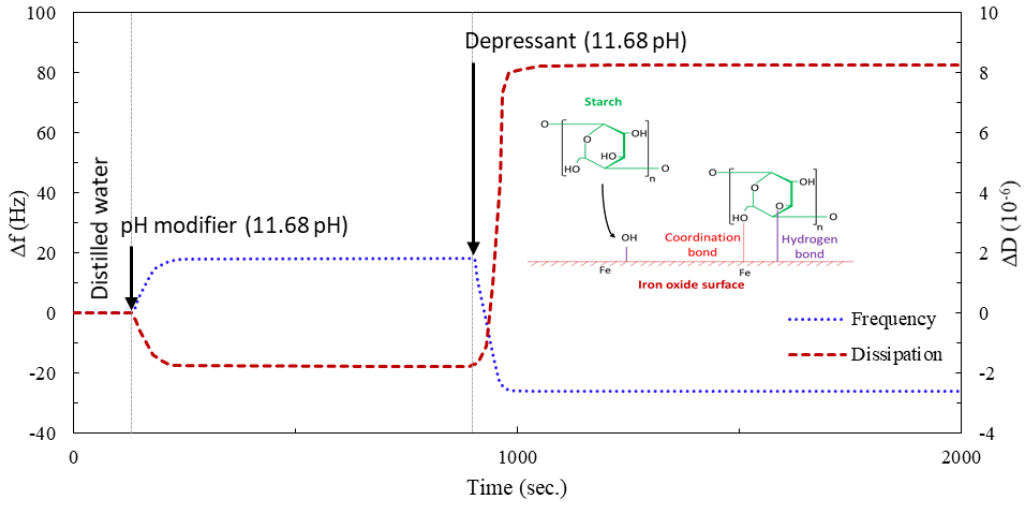

Fig. 10. Frequency and dissipation shafts with time as a result of interactions of pH modifier (NaOH) followed by starch depressant (starch) with the surface of iron oxide studied by *QCM-D*

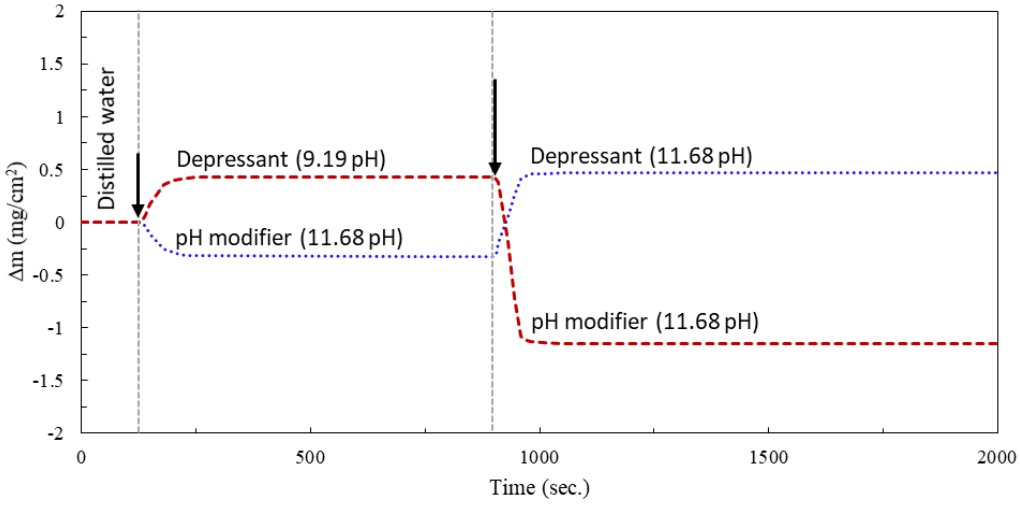

Fig. 11. The Sauerbrey mass shift on iron oxide sensor during *QCM-D* experiments conducted with different reagent addition sequences

ption then decreased to -1.15 mg/cm^2 by the addition of pH modifier. In the other case, using the pH regulator decreased Δm to -0.32 mg/cm^2, which increased to 0.46 mg/cm^2 upon the addition of starch solution.

In summary, *QCM-D* analysis results are consistent with the flotation test results, which for a more efficient flotation process, the pH modifier is added prior to the addition of the starch solution, so that starch molecules cover the iron oxide particles and prevent the subsequent adsorption of the anionic collector in the reverse flotation of iron oxide minerals. Also, Veloso et al. (2018) found that corn starch showed the best depression performance at pH larger than 10.5.

4. Conclusions

Regardless of the reagents addition sequence, the higher separation performance was obtained at 1.6 kg/Mg starch dosage, but at that dosage, the separation efficiency was greater by 21% when the pH regulator was used prior to the starch addition to the flotation feed, and the concentrate Fe grade and recovery were obtained as 69.5% and 83.5%, respectively. *QCM-D* results showed that the addition of starch solution prior to the strong alkaline solution reduced the adsorption of starch on the iron oxide chip, which in consequence reduced the separation performance. Under strong alkaline conditions, *QCM-D* confirmed that starch molecules covered the surface of iron oxide minerals and prevented the subsequent adsorption of the anionic collector in the reverse flotation of iron oxide minerals. Comprehensive analysis of *QCM-D* and flotation experiments results confirmed that the addition of pH regulator prior starch showed a superior positive impact on the reverse flotation efficiency.

References

BHAGYALAXMI, K., HRUSHIKESH, S., SWAGAT, S.R., DAS, B., 2103. *Investigations on different starches as depressants for iron ore flotation*. Minerals Engineering, 49, 1-6.

BOUCHET-SPINELLI, A., COCHE-GUERENTE, L., ARMAND, S., LENOUVEL, F., LABBE, P., FORT, S., 2013. *Functional characterization of starch-degrading enzymes using quartz crystal microbalance with dissipation monitoring (QCM-D)*. Sensors and Actuators B: Chemical, 176, 1038–1043.

BUTT, H.J., CAPPELLA, B., KAPPL, K., 2005. *Force measurements with the atomic force microscope: Technique, interpretation and applications*. Surface Science Reports, 59(1–6), 1-152.

CLEGG, J., LUDOLPH, C.M., PEPPAS, N.A., 2019. *QCM-D assay for quantifying the swelling, biodegradation, and protein adsorption of intelligent nanogels*. Journal of Applied Polymer Science, 137(25), 48655.

FILIPPOV, L.O., SEVEROV, V.V., FILIPPOVA, I.V., 2014. *An overview of the beneficiation of iron ores via reverse cationic flotation*. International Journal of Mineral Processing, 127, 62-69.

HODGES, C.S., HARBOTTLE, D., BIGGS, S., 2020. *Investigating adsorbing viscoelastic fluids using the quartz crystal microbalance*. American Chemical Society ACS Omega, 5(35), 22081–22090.

ISHIKAWA, A., YOSHIOKA, T., SATO, T., OKUWAKI, A., 1997. *Solubility of hematite in LiOH, NaOH and KOH solutions*. Hydrometallurgy, 45(1–2), 129-135.

KONRADI, R., TEXTOR, M., REIMHULT, E., 2012. *Using complementary acoustic and optical techniques for quantitative monitoring of biomolecular adsorption at interfaces*. Biosensors, 2(4), 341-376.

LIN, Y., HUANG, Q., SU, Z., 2010. *Interaction between protein and polysaccharide studied by QCM-D[J]*. Chinese Journal of Applied Chemistry, 27(5): 505-509.

LU, D., HU, Y., LI, Y., JIANG, T., SUN, W., WAND, Y., 2017. *Reverse flotation of ultrafine magnetic concentrate by using mixed anionic/cationic collectors*. Physicochemical Problems of Mineral Processing, 53(2), 724-736.

QUAST, K., 2017. *Literature review on the use of natural products in the flotation of iron oxide ores*. Minerals Engineering, 108, 12–24.

MA, M., 2012. *Froth flotation of iron ores*. International Journal of Mining Engineering and Mineral Processing, 1(2), 56-61.

REN, A.J., SUN, C.Y., 2018. *Effect of modified starches on floatability of hematite and quartz using sodium oleate as collector*. Mining and Metallurgy. 27(3), 1-12 (In Chinese).

SAKAI K., 2019. *Quartz crystal microbalance with dissipation monitoring (QCM-D)*. In: Abe M. (eds) Measurement Techniques and Practices of Colloid and Interface Phenomena. Springer, Singapore.

SAFTICS, A., PROSZ, G., TURK, B. PETER, B., KURUNCZI, S., HORVATH, R., 2018. *In situ viscoelastic properties and chain conformations of heavily hydrated carboxymethyl dextran layers: a comparative study using OWLS and QCM-I chips coated with waveguide material*. Scientific Report, 8, 11840.

SYLVESTER, P.J., 2012. *Chapter 1: Use of the mineral liberation analyzer (MLA) for mineralogical studies of sediments and sedimentary rocks*. Mineralogical Association of Canada Short Course 42, St. John's NL, May 2012, 1-16. https://www.researchgate.net/publication/240305728_Use_of_the_Mineral_Liberation_Analyzer_MLA_for_mineralogical_studies_of_sediments_and_sedimentary_rocks

TAO, D., WU, Z., SOBHY, A., 2021. *Investigation of nanobubble enhanced reverse anionic flotation of hematite and associated mechanisms*. Powder Technology, 379, 12-25.

TOHRY, A., DEHGHAN, R., CHELGANI, S.C., ROSENKRANZ, J., RAHMANI, O.A., 2019. *Selective separation of hematite by a synthesized depressant in various scales of anionic reverse flotation*. Minerals, 9(2), 124.

VELOSO, C.H., FILIPPOV, L.O., FILIPPOVA, I.V., ARAUJO, A.C., 2018. *Investigation of the interaction mechanism of depressants in the reverse cationic flotation of complex iron ores*. Minerals Engineering, 125, 133–139.

VIJAYAKUMAR, T.V., RAO, D.S., RAO, S.S., PRABHAKAR, S., RAJU, G.B., 2010. *Reverse flotation studies on an Indian low grade iron ore slimes*. International Journal of Engineering Science and Technology, 2(4), 637-648.

WANG, S., ALAGHA, L., XU, Z., 2014. *Adsorption of organic–inorganic hybrid polymers on kaolin from aqueous solutions*. Colloids and Surfaces A: Physicochemical and Engineering Aspects, 453, 13-20.

WEISSENBORN, P.K., 1996. *Behaviour of amylopectin and amylose components of starch in the selective flocculation of ultrafine iron ore*. International Journal of Mineral Processing, 47(3–4), 197-211.

YANG, S., WANG, L., 2018. *Structural and functional insights into starches as depressant for hematite flotation*. Minerals Engineering, 124, 149–157.

YANG, S., LI, C., WANG, L., 2017. *Dissolution of starch and its role in the flotation separation of quartz from hematite*. Powder Technology, 320, 346-357.

ZHANG, M., PAN, G., ZHAO, D., HE, G., 2011. *XAFS study of starch-stabilized magnetite nanoparticles and surface speciation of arsenate*. Environmental Pollution 159, 3509-3514.

ZHANG, Y., HE, Y., ZHANG, T., ZHU, X., FENG, Y., ZHANG, G., BAI, X., 2018. *Application of Falcon centrifuge in the recycling of electrode materials from spent lithium ion batteries*. Journal of Cleaner Production, 202, 736-747.